nature chemistry

SUPPLEMENTARY INFORMATION

DOI: 10.1038/NCHEM.1570

Molecular tweezers modulate 14-3-3 protein-protein interactions

David Bier[1,#], Rolf Rose[1,#], Kenny Bravo-Rodriguez[2], Maria Bartel[1], Juan Manuel Ramirez-Anguita[2], Som Dutt[3], Constanze Wilch,[3] Frank-Gerritt Klärner[3], Elsa Sanchez-Garcia[2], Thomas Schrader[3], Christian Ottmann[1]*

[1]Chemical Genomics Centre of the Max-Planck-Society, Otto-Hahn-Strasse 15, 44227 Dortmund, Germany

[2]Max-Planck-Institut für Kohlenforschung, Kaiser-Wilhelm-Platz 1, 45470 Mülheim an der Ruhr, Germany

[3]Department of Chemistry, University of Duisburg-Essen, Universitätsstrasse 7, 45117 Essen, Germany

Table of Contents

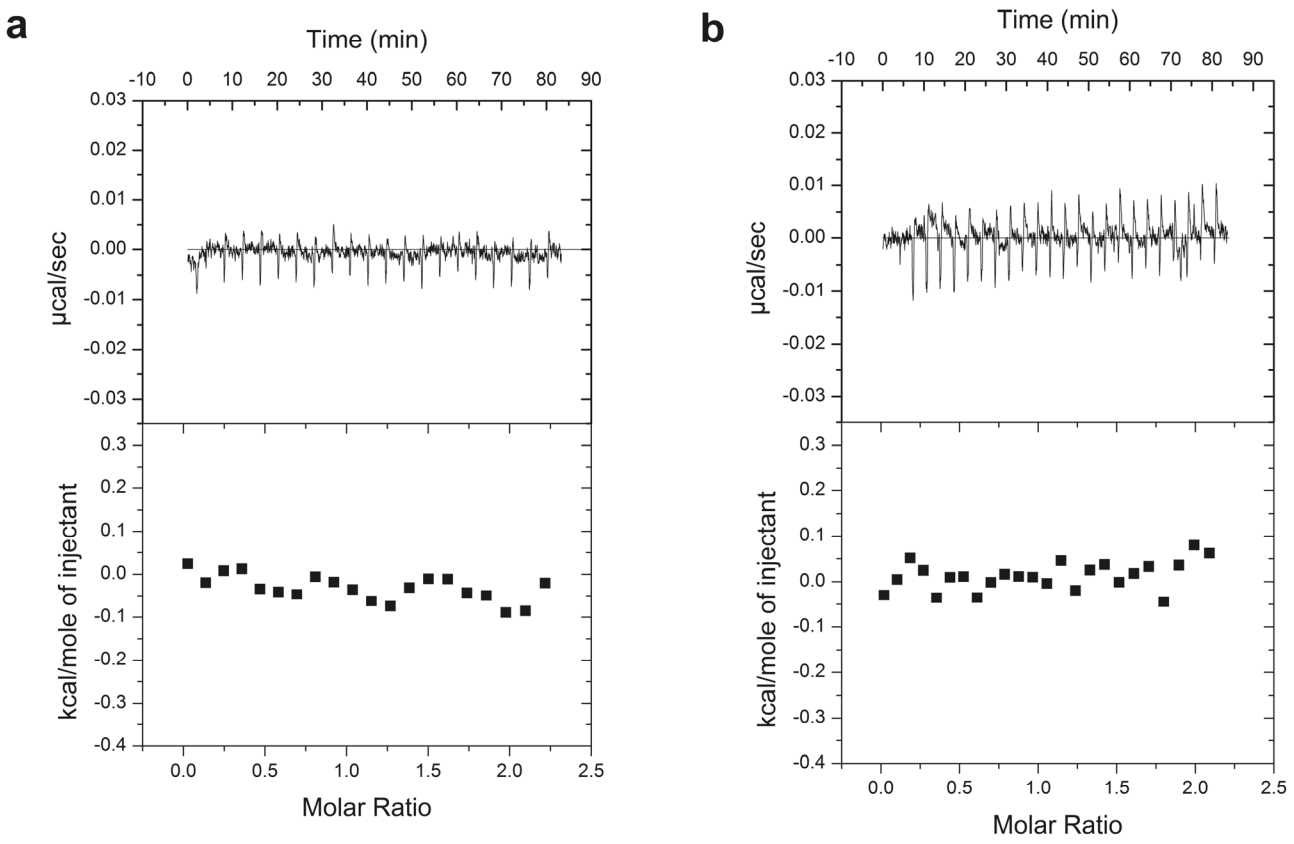

Supplementary Figure S1: Isothermal Titration Calorimetry (ITC) control experiments. **a)** Titration of 20 mM MES (morpholineethanesulfonic acid) (pH 6.5) and 2 mM $MgCl_2$ to 50µM 14-3-3σ solved in the same buffer. **b)** Titration of 500µM molecular tweezers dissolved in 20 mM MES (morpholineethanesulfonic acid) (pH 6.5) and 2 mM $MgCl_2$ to the same buffer.

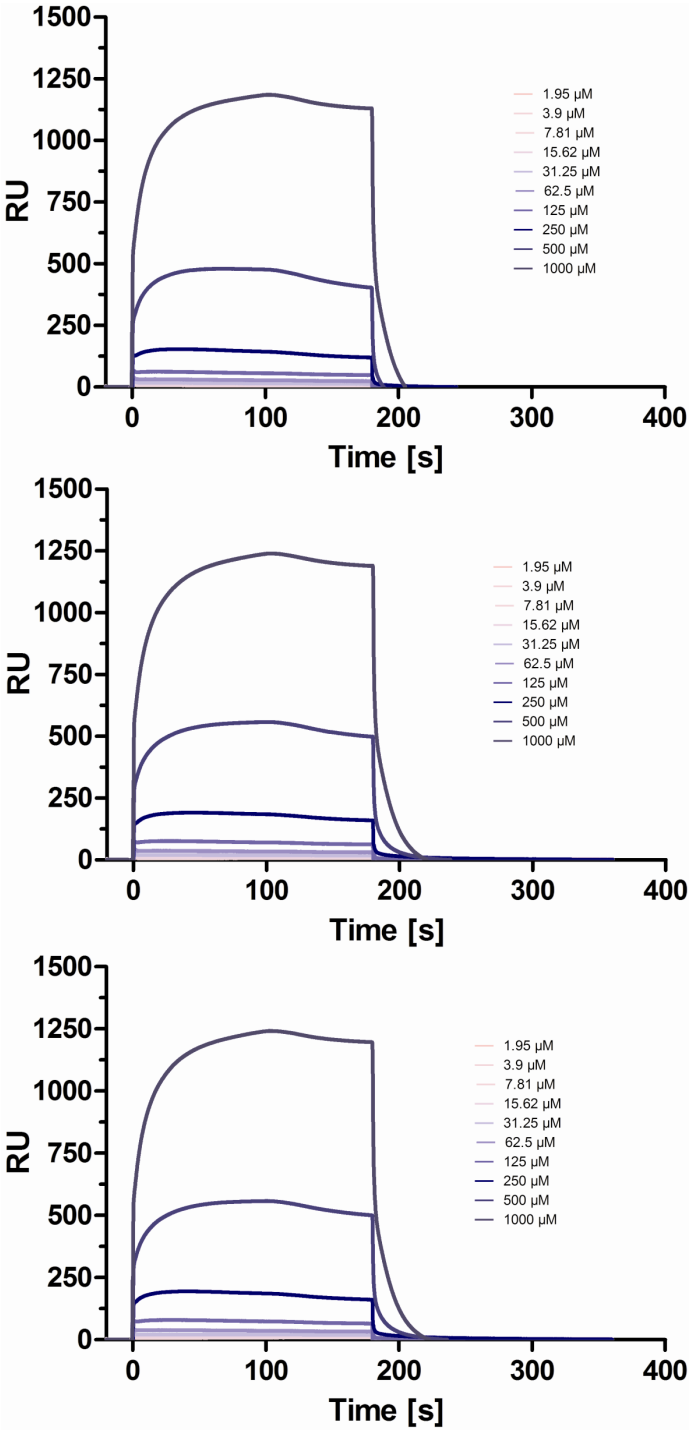

Supplementary Figure S2. Surface plasmon resonance analysis of the tweezers binding to immobilized 14-3-3σ. Three independent experiments are shown.

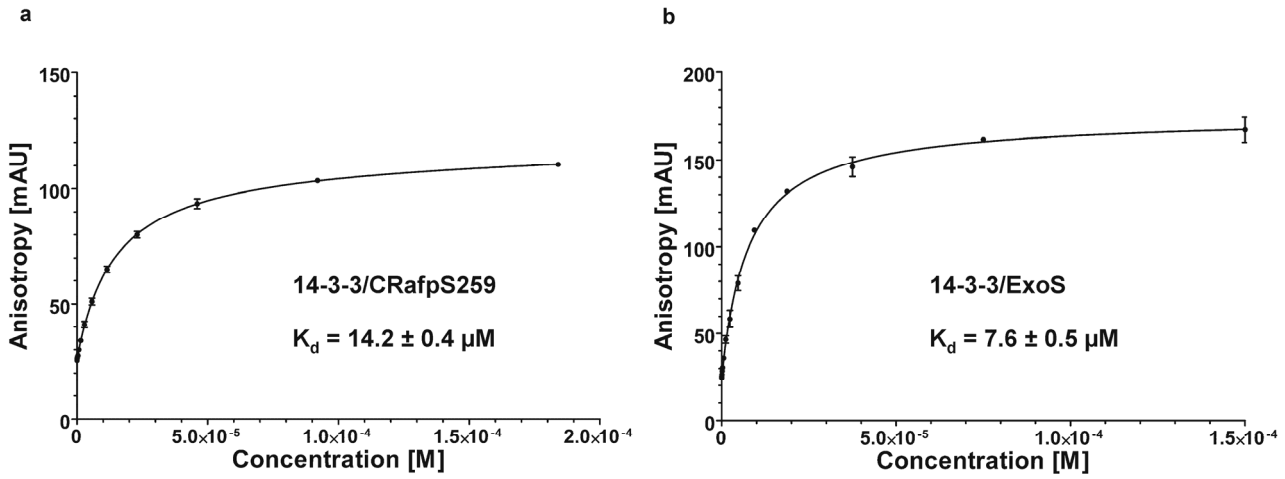

Supplementary Figure S3. Fluorescence polarisation (FP) with CRafpS259 or ExoS binding to 14-3-3σ. a) Binding of the FAM-labelled synthetic CRafpS259 peptide (FAM-^{255}QRSTpSTPNVH^{264}-COOH) to purified 14-3-3ζ measured by FP. The measured anisotropy r is plotted in mAU against the 14-3-3 concentration. Each data point is the average of a triplicate measurement including the standard deviation (error bars). The continuous line corresponds to the non-linear regression of the fit. The measured K_d values for each titration are displayed and represent the average of three independent measurements. **b)** Binding of the FAM-labelled synthetic ExoS peptide (FAM-^{416}SGHGQGLLDALDLAS^{430}) to purified 14-3-3ζ measured by FP.

X-ray data collection, structure determination and refinement. In the case of the 3.2-Å structure, data collection was performed inhouse on a rotating copper anode (Nonius, wavelength 1.5418 Å). The data collection for the 2.35-Å structure was performed at the Swiss Light Source (SLS, beamline PXII, wavelength 1.0400 Å). Data were processed with XDS[1]. Molecular replacement was carried out with PHASER[2] and the 14-3-3σ structure (PDB code 1YWT) was used as the search model. The obtained model was subjected to iterative rounds of model building and refinement using the programs COOT[3] and REFMAC[4]. Figures were prepared with PYMOL (www.pymol.org).

1. Kabsch, W. XDS. *Acta Crystallogr. D, Biol. Crystallogr.* **66**, 125-32 (2010).
2. McCoy, A. J. et al. Phaser crystallographic software. *J. Appl. Crystallogr.* **40**, 658-674 (2007).
3. Emsley, P. & Cowtan, K. Coot: model-building tools for molecular graphics. *Acta Crystallogr. D, Biol. Crystallogr.* **60**, 2126-32 (2004).
4. Murshudov, G. N., Vagin, A. A. & Dodson, E. J. Refinement of macromolecular structures by the maximum-likelihood method. *Acta Crystallogr. D, Biol. Crystallogr.* **53**, 240-55 (1997).

Supplementary Table S1. Data collection and refinement statistics (3.2-Å complex, PDB ID 4HRU)

	14-3-3σ/Tweezers[#]
Data collection	
Space group	C222
Cell dimensions	
a, b, c (Å)	63.49, 154.77, 77.02
α, β, γ (°)	90.0, 90.0, 90.0
Resolution (Å)	20.0 - 3.2 (3.5 - 3.2)
Rmerge	13.0 (28.3)
I / σI	15.94 (6.57)
Completeness (%)	99.3 (99.9)
Redundancy	3.52 (3.61)
Refinement	
Resolution (Å)	19.58 – 3.2
No. reflections	6195
Rwork / Rfree	0.23 / 0.31
No. atoms	
Protein	1752
Ligand/ion	52
B-factors	
Protein	30.98
Ligand/ion	46.12
R.m.s. deviations	
Bond lengths (Å)	0.012
Bond angles (°)	1.718

#Data were collected from a single crystal. Values in parentheses are for highest-resolution shell.

Supplementary Table S2. Data collection and refinement statistics of the 14-3-3σ/Tweezers structure (2.35-Å complex, PDB ID 4HQW)

	14-3-3σ/Tweezers[#]
Data collection	
Space group	C222
Cell dimensions	
a, *b*, *c* (Å)	60.40, 157.40, 77.20
α, β, γ (°)	90.00, 90.00, 90.00
Resolution (Å)	45.54-2.35 (2.41-2.35)
R_{merge}	5.6 (33.5)
$I / \sigma I$	22.44 (4.74)
Completeness (%)	99.94 (100)
Redundancy	15.96 (16.70)
Refinement	
Resolution (Å)	45.54-2.35 (2.41-2.35)
No. reflections	14955
R_{work} / R_{free}	0.1835/0.2436 (0.1804/0.2448)
No. atoms	
Protein	1811
Ligand/ion	51/5
Water	186
B-factors	
Protein	58.61
Ligand/ion	77.58
Water	78.92
R.m.s. deviations	
Bond lengths (Å)	0.0178/0.0175
Bond angles (°)	1.9215/1.9169

#Data were collected from a single crystal.
Values in parentheses are for highest-resolution shell.

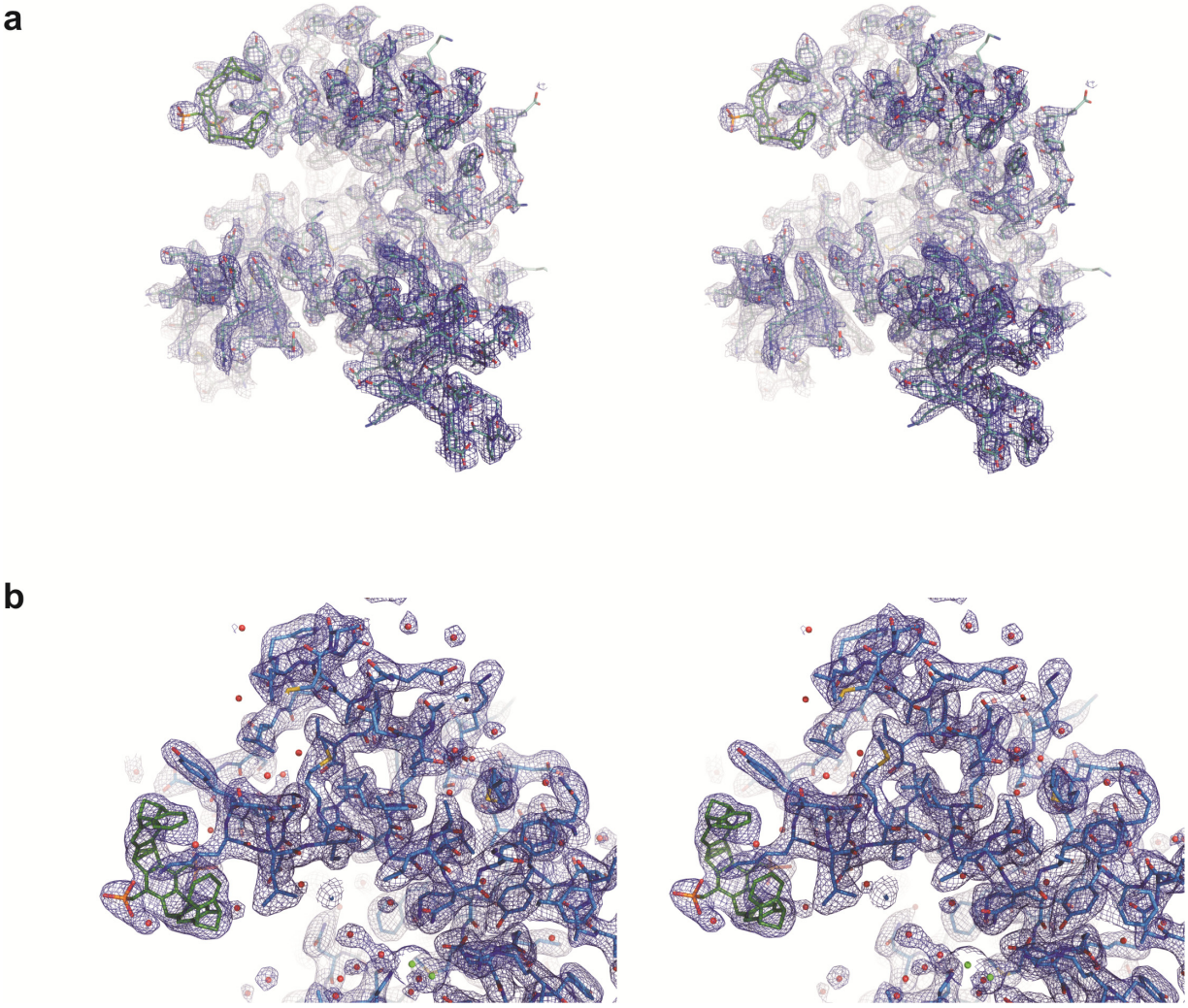

Supplementary Figure S4. a) Stereo figure of the 2Fo-Fc electron density of the 3.2-Å 14-3-3σ/tweezers complex. 2Fo-Fc electron density map covering the complete 14-3-3σ monomer. The 14-3-3σ protein is shown as a stick model in blue, the tweezers is displayed as a stick model in green. **b)** Stereo figure of the 2Fo-Fc electron density of the 2.35-Å 14-3-3σ/tweezers complex. 2Fo-Fc electron density map covering the complete 14-3-3σ monomer. The 14-3-3σ protein is shown as a stick model in blue, the tweezers is displayed as a stick model in green.

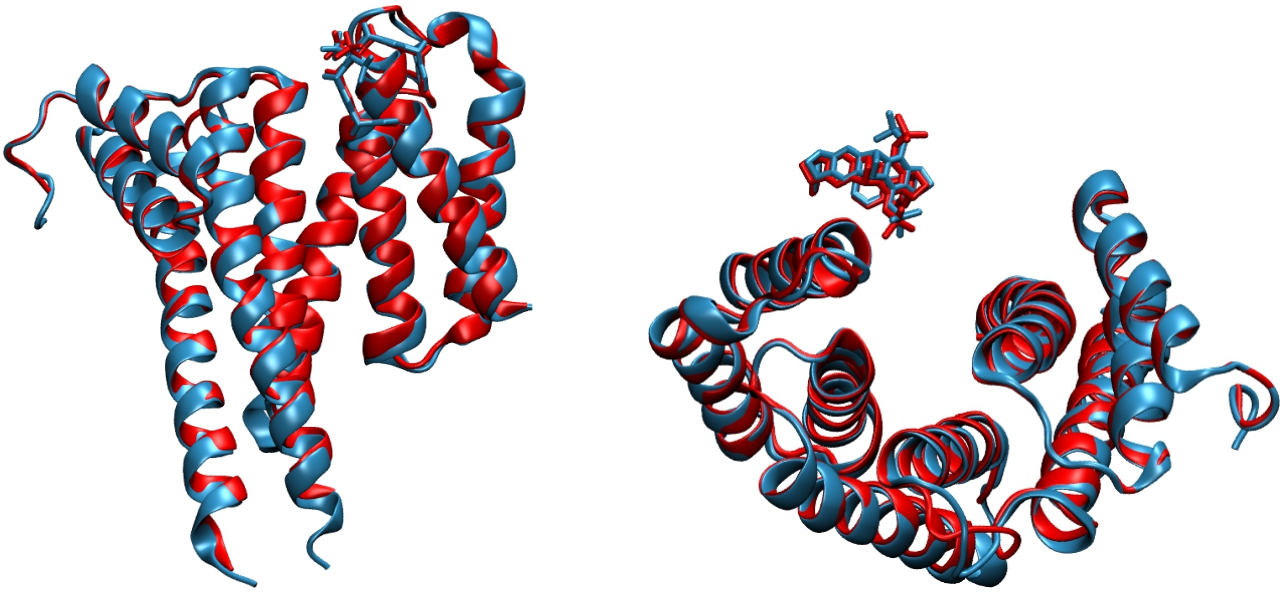

Supplementary Figure S5. Superimposition of both crystal structures (3.2 Å red and 2.35 Å blue). Left: Side view; right: top view. Note the opposite orientation of the tweezers' remote phosphate moiety, which points to Arg224' (red) or to the included Lys214 ammonium ion (blue). RMSD value for the alignment is 0.710 Å.

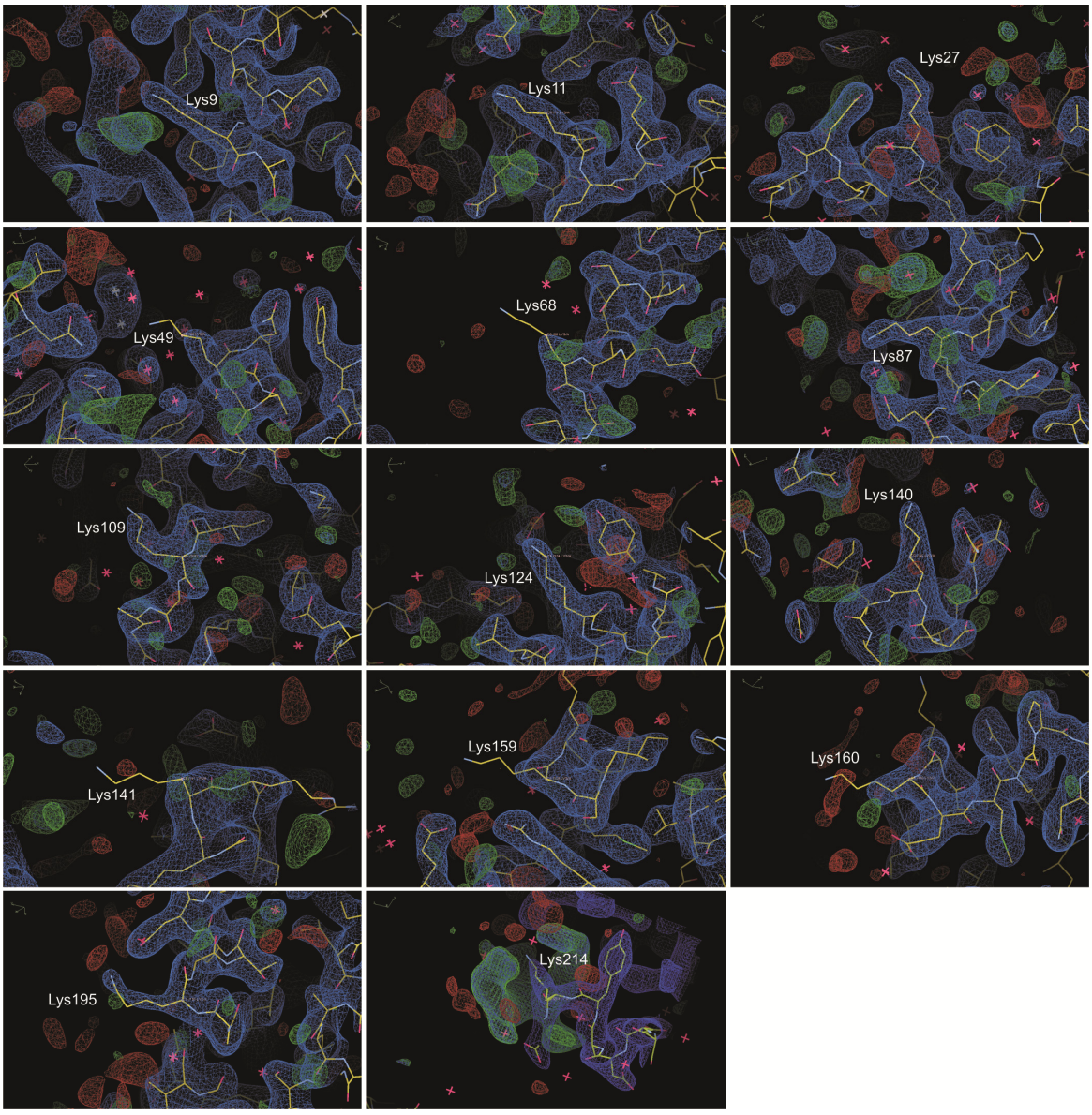

Supplementary Figure S6. Electron density surrounding surface-exposed lysines in 14-3-3σ. The initial 2Fo-Fc (blue mesh, contoured at 1σ) and Fo-Fc (green and red mesh, contoured at 2.5 σ) electron density maps surrounding the model of 14-3-3σ (yellow sticks) are shown. No tweezers molecule had been added to the model at this stage. With the exception of the site at Lys214 no density could be observed in the vicinity of the other surface-exposed lysines that could be interpreted as an additional tweezers molecule.

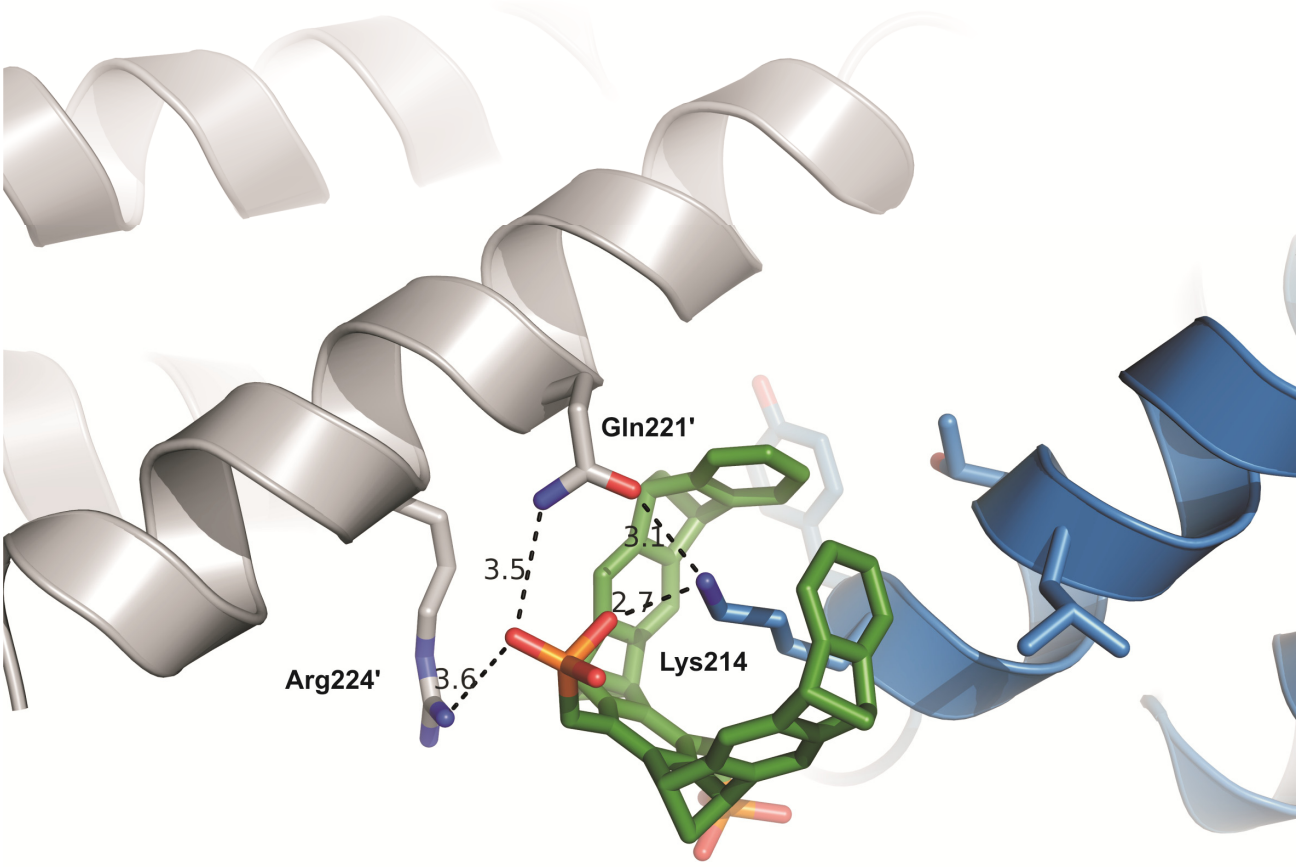

Supplementary Figure S7. Coordination of one tweezers' phosphate moiety by Gln221 and Arg224 from a symmetry-related 14-3-3 protein. The phosphate moiety of the molecular tweezers (green, orange and red sticks) engages the ε-amino group of Lys214 (lightblue and blue sticks) and makes additional polar contact (black dashed line) with Gln 221´ and Arg224´ (lightgrey and blue) from a symmetry-related 14-3-3σ monomer (lightgrey cartoon).

Computational details. The initial set of protein coordinates used for the MD simulations was taken from the X-ray structure of the 14-3-3σ protein (PDB code: 1YZ5) which was also used to build the missing loops formed by residues 68 to 77 and 137 to 139. The protonation states of titratable side chains were determined using the web interface of the PROPKA 2.0 software[1,2] and the missing hydrogen atoms were added with the PDB2PQR program.[3] The parameters for the dihydrogen-phosphate tweezers were generated using the Swissparam server[4] and their suitability tested by us.

Each of the 17 lysine residues in 14-3-3 was placed inside the cavity of the dihydrogen-phosphate tweezers and the resulting complexes were submitted to an energy minimization using CHARMM.[5,6] The minimized structures were then solvated with a water box with 65x80x80 Å size and neutralized using VMD 1.9.[7] The solvated systems were subjected to a 100 ps NVT molecular dynamics (MD) simulation with the tweezers and protein atoms frozen. After that, a 100 ps NPT MD simulation was carried out with only the backbone atoms of the protein fixed. Finally, a 40 ns production MD simulation was performed. All MD simulations were done with the NAMD 2.7 program.[8] The CHARMM 22 force field[9] was used for all atoms (TIP3P model for the water environment).[10]

QM/MM optimizations of three randomly selected snapshots (chosen close in time to each other and towards the end of the simulation to minimize the effect of structural fluctuations) from the MD simulations were performed with the program ChemShell v3.4.[11] We used Turbomole 5.10[12] for the QM calculations and DL_POLY[13] as driver of the CHARMM22 force field. The QM part which includes all atoms of the tweezers and part of lysine (Supplementary Figure S8) was described using the B3LYP density functional with empirical dispersive energy correction (B3LYP-D2)[14-16] and the SVP basis set from the Turbomole basis set library. Open valencies at the QM/MM border were saturated using hydrogen link atoms.[17] We applied an electrostatic embedding scheme.[18] To avoid overpolarization of the QM region at the boundary a charge shift scheme was applied.[19,20] No electrostatic cutoffs were used. The optimization was performed with the HDLC optimizer.[21] The active region consisted of a 1000 atoms sphere centered on the nitrogen atom of the lateral chain of lysine (NZ). All atoms within the active region were allowed to move in each optimization step. The optimization was finished when the maximum gradient component was below 0.00045 a.u.

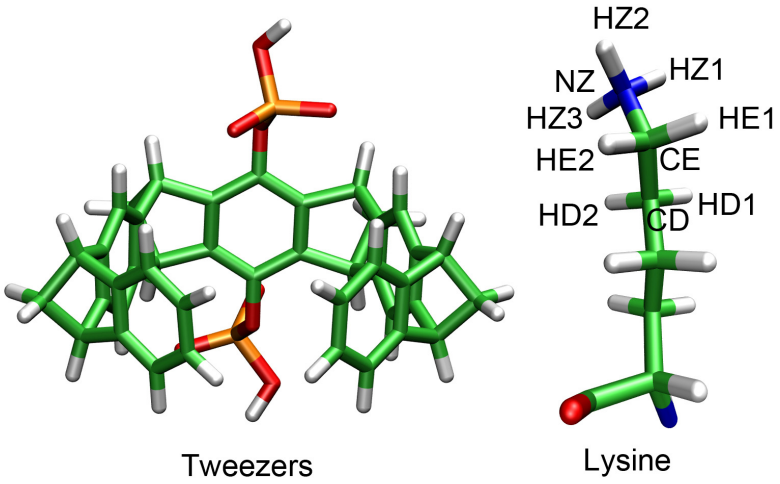

Supplementary Figure S8. The QM region includes all atoms of the tweezers and the NZ, HZ1, HZ2, HZ3, CE, HE1, HE2, CD, HD1 and HD2 atoms of lysine.

Supplementary Table S3. Average values of selected distances and angles during the MD simulations indicate how "open" the tweezers is (Cp-Cp' and Cm-Cm' distances), how close the lysine is to the tweezers hydrogen-phosphate group and how deeply it is placed inside the cavity of the tweezers (N-P distance and C-C1-N angle, respectively). The most relevant conserved interactions with nearby residues are also shown.

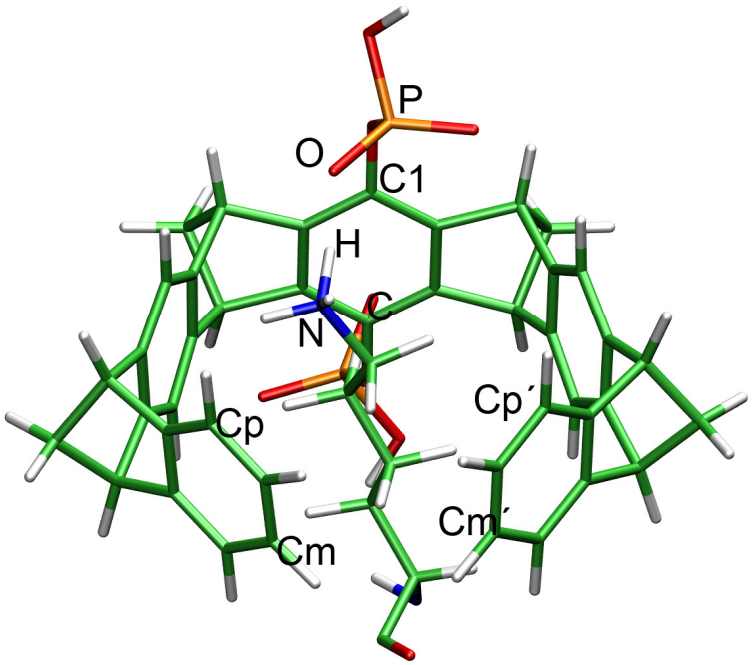

LYS	Cp-Cp' (Å)	Cm-Cm' (Å)	N-P (Å)	C-C1-N (°)	Interaction with nearby amino acids
141	5.99 ± 0.58	4.41 ± 0.63	3.97 ± 0.19	91.9 ± 7.7	1.90 ± 0.67 (Arg142)
87	6.30 ± 0.95	4.91 ± 0.95	-	74.6 ± 9.4	-
160	5.65 ± 0.47	4.09 ± 0.46	4.00 ± 0.16	86.8 ± 4.9	-
214*	5.78 ± 0.45	4.14 ± 0.45	3.97 ± 0.15	88.5 ± 5.3	*
195	5.85 ± 0.50	4.09 ± 0.54	3.98 ± 0.14	86.1 ± 4.6	-
159	5.64 ± 0.38	4.00 ± 0.36	3.94 ± 0.14	88.8 ± 4.9	
109	5.76 ± 0.48	4.25 ± 0.50	3.97 ± 0.15	88.4 ± 5.0	-
27	5.69 ± 0.33	4.05 ± 0.34	3.98 ± 0.14	86.5 ± 3.8	2.19 ± 0.51 (Ala24)
11	6.43 ± 0.70	4.95 ± 0.78	3.94 ± 0.18	88.9 ± 8.5	1.83 ± 0.14 (Ala10)
68	5.76 ± 0.36	4.10 ± 0.38	3.96 ± 0.15	87.6 ± 5.0	1.96 ± 0.23 (Ile65)
49	5.65 ± 0.33	3.93 ± 0.31	3.97 ± 0.14	87.7 ± 4.5	1.71 ± 0.12 (Tyr127)
140	5.51 ± 0.33	3.96 ± 0.32	4.03 ± 0.15	82.9 ± 4.6	-
9	8.52 ± 0.81	7.47 ± 0.92	4.1 ± 0.67	56.4 ± 4.8	-
124	6.42 ± 1.45	5.18 ± 1.50	3.91 ± 0.17	51.3 ± 4.4	-

* Along the MD simulation one of the phosphates groups interacts either with Glu210 or Asp211

Supplementary Table S4. Selected distances and angles for the snapshots optimized at the QM/MM level (QM(B3LYP-D2/SVP)/CHARMM).

LYS	Snapshots	Cp-Cp' (Å)	Cm-Cm' (Å)	O-H (Å)	C-C1-N (°)	Interaction of the tweezer with nearby amino acids	
141	1	5.50	3.73	1.62	99.5	1.67 (Arg142)	2.39 (Arg142)
	2	5.45	3.92	1.61	94.6	1.71 (Arg142)	1.90 (Arg142)
	3	5.45	3.95	1.63	91.9	1.73 (Arg142)	1.99 (Arg142)
87	1	7.41	5.76	-	83.0		
	2	5.79	4.20	-	90.3		
	3	4.99	3.60	-	75.2		
160	1	5.18	3.63	1.56	89.4	1.55 (Glu161)	
	2	5.99	4.06	1.59	80.6	1.57 (Glu161)	
	3	5.45	3.89	1.60	86.1	1.54 (Glu161)	
214	1	5.25	3.67	-	81.3	1.85 (Gln210)	
	2	5.98	3.98	1.61	100.4	1.62 (Gln210)	
	3	5.38	3.75	1.56	92.8	1.83 (Gln210)	
195	1	5.51	3.74	1.55	82.1	1.79 (Thr196)	
	2	5.55	3.7	1.54	85.9	1.78 (Thr196)	
	3	5.55	3.63	1.56	87.6	1.75 (Thr196)	
159	1	5.10	3.60	1.49	84.1		
	2	5.36	3.70	1.53	90.4		
	3	5.22	3.64	1.61	84.9		
109	1	5.41	4.29	1.56	91.2	1.57 (Glu110)	
	2	5.64	4.09	1.56	86.2	1.58 (Glu110)	
	3	5.34	3.88	1.52	92.3	-	
27	1	5.23	3.62	1.51	85.9	2.10 (Met-2)	
	2	5.29	3.67	1.64	89.0	1.72 (Met-2)	
	3	5.58	3.66	1.57	89.3	1.61 (Met-2)	
11	1	5.76	3.90	1.59	95.8	1.77 (Lys11)	1.80 (Ala10)
	2	7.33	5.38	1.52	96.5	1.79 (Lys11)	2.09 (Ala10)
	3	5.59	3.65	1.54	98.0	1.80 (Lys11)	1.81 (Ala10)
68	1	5.36	3.56	1.61	89.0	1.61 (Lys77)	2.27 (Ile65)
	2	5.13	3.58	1.77	79.0	1.59 (Lys77)	1.70 (Ile65)
	3	5.42	3.77	1.58	88.0	1.57 (Lys77)	1.71 (Ile65)
49	1	5.58	3.61	1.59	84.1	1.60 (Lys122)	1.75 (Tyr127)
	2	5.65	3.57	1.56	85.0	1.60 (Lys122)	1.66 (Tyr127)
	3	5.59	3.75	1.63	86.4	1.61 (Lys122)	1.68 (Tyr127)
140	1	5.22	3.65	1.60	82.3	-	
	2	5.35	3.58	1.65	87.2	2.30 (Gly137)	
	3	5.03	3.51	1.72	85.0	1.85 (Gly137)	
9	1	7.87	6.54	1.56	54.7		
	2	8.83	7.77	1.67	58.1		
	3	9.27	8.25	1.62	58.6		
124	1	5.30	3.95	1.60	51.2	1.69 (Tyr128)	1.75 (Cys96)
	2	5.11	3.82	1.59	53.0	1.69 (Tyr128)	1.72 (Cys96)
	3	5.39	3.83	1.55	52.0	1.66 (Tyr128)	1.71 (Cys96)

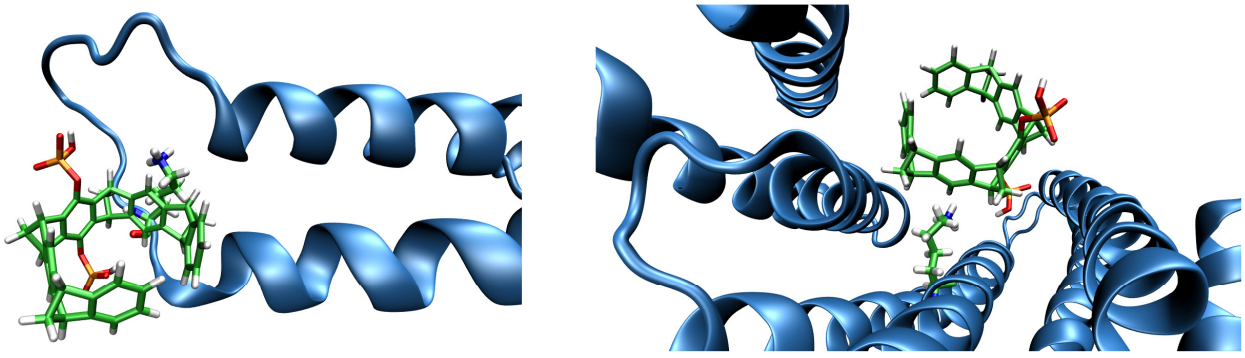

Supplementary Figure S9. Lys77 and Lys122 are not accessible for the tweezers. Lys77 is pointing towards the interior of one of the loops connecting the α-helixes of the protein and is involved in hydrogen bond interactions with polar residues while Lys122 is buried in the central channel of the protein.

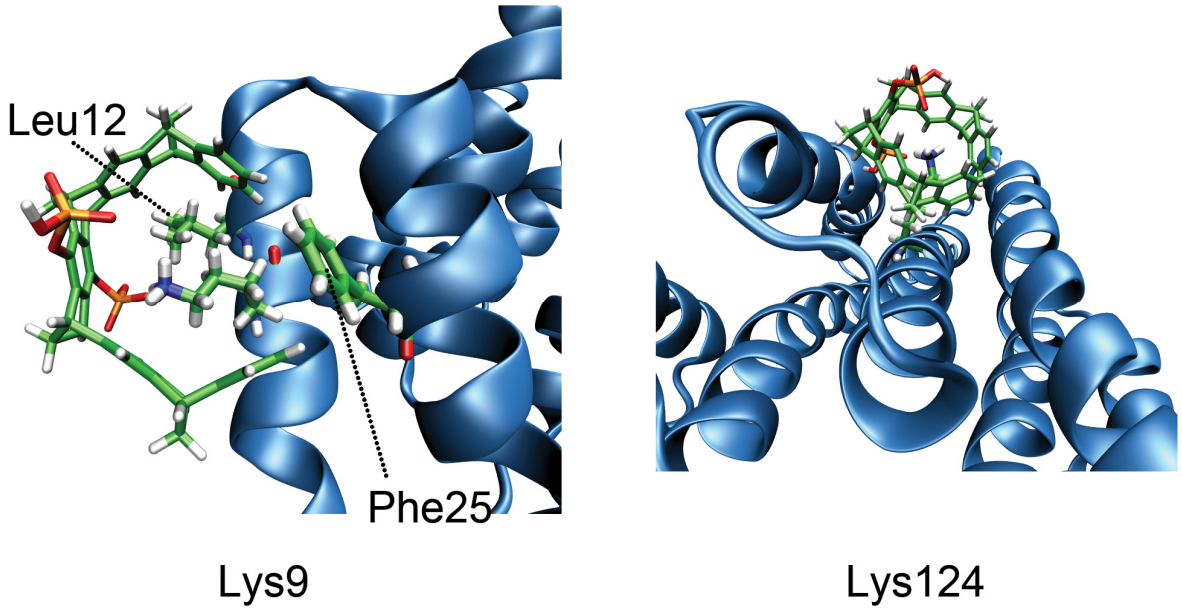

Supplementary Figure S10. Steric hindrance for Lys124 and Lys9 (Rule 1). Lys124 is buried within two alpha helices; tweezers insertion is possible but severely hindered. In Lys9 the disposition of the lateral chains of surrounding amino acids result in Phe25 being placed in front of the tweezers while Leu12 is situated near one of its hydrogen-phosphate groups and below the plane defined by the carbon atoms of the tweezers. Under these conditions, the tweezers is deformed to a much stressed “open” conformation and Lys9 cannot be properly accommodated inside its cavity as shown by the small values of the C-C1-N angle and the large Cp-Cp' and Cm-Cm' distances (Tables S3 and S4).

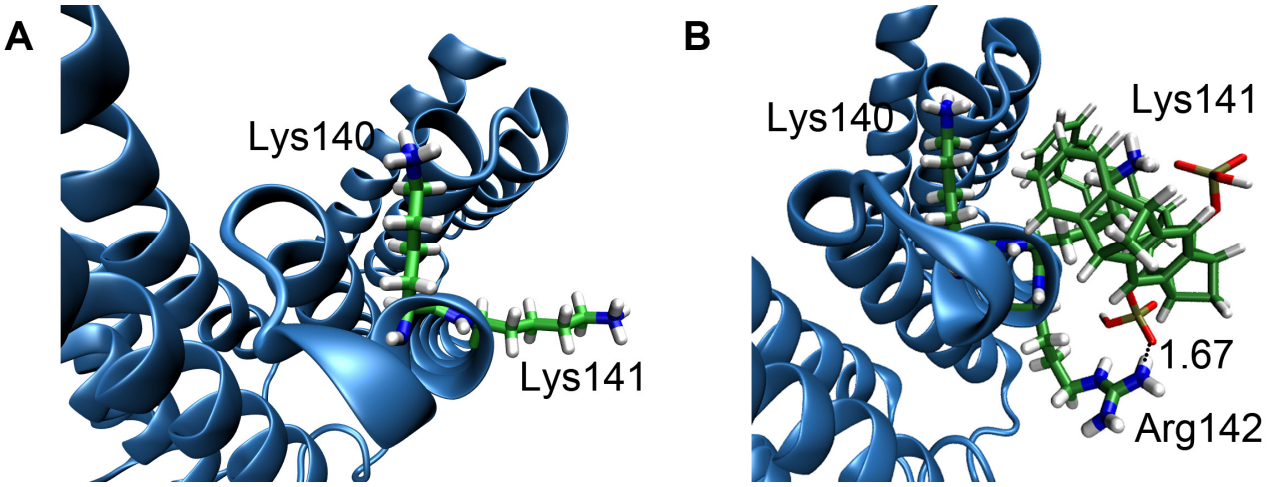

Supplementary Figure S11. Additional ion pair with Arg142 on complexation of Lys141 (Rule 2). Although Lys140 and Lys141 are consecutive residues their different protein environments explain the different stabilities of their QM regions: Lys140 points towards the neighbor alpha helix, while Lys141 is exposed (A, Rule 1). Most importantly, Lys141 complexation also allows formation of a strong additional salt bridge between its hydrogen phosphate and Arg142 (B, Rule 2).

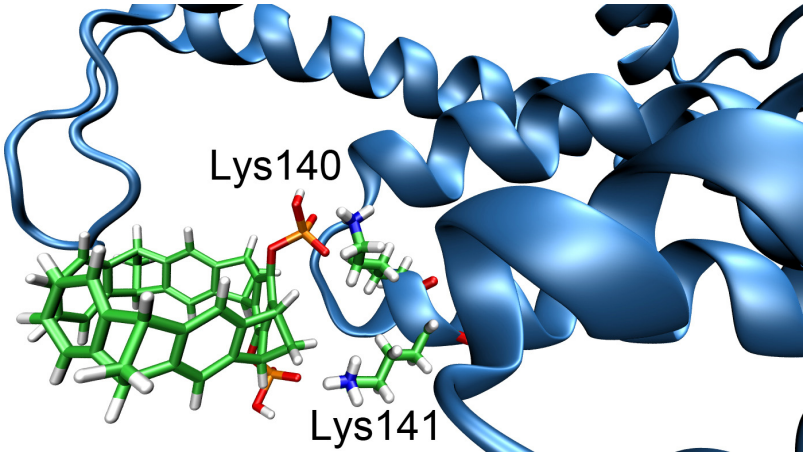

Supplementary Figure S12. Lys140 and Lys141 can also be involved in multiple competing external salt bridges (Rule 3). When Lys140 and Lys141 are close but not inside the tweezers cavity, the tweezer is "diverted" during the MD simulation from locking a lysine inside its cavity to form two salt bridges between its hydrogen phosphate groups and both ammonium cations.

214-t.wmv and 141-t.wmv: Molecular dynamics simulations of complex formation between 14-3-3 and the molecular tweezers described in this manuscript. 214-t.wmv: dynamic nature and kinetic stability (40 ns) of the side chain inclusion from Lysine-214 inside the molecular tweezers; 141-t.wmv: cooperative threading of Lys-141 into the tweezers cavity reinforced by external ion pair formation with a proximal arginine (40 ns).

SUPPORTING REFERENCES

1. Li, H., Robertson, A.D. & Jensen, J.H. Very fast empirical prediction and rationalization of protein pKa values. *Proteins: Struct., Funct., Bioinf.* 61, 704-721 (2005).
2. Bas, D.C., Rogers, D.M. & Jensen, J.H. *Proteins* 73, 765-783 (2008).
3. Dolinsky T.J, Nielsen J.E, McCammon J.A & N.A., B. PDB2PQR: an automated pipeline for the setup, execution, and analysis of Poisson-Boltzmann electrostatics calculations. *Nucleic Acids Research* 32 W665-W667 (2004).
4. Zoete, V., Cuendet, M.A., Grosdidier, A. & Michielin, O. SwissParam: A Fast Force Field Generation Tool for Small Organic Molecules. *J. Comp. Chem.* 32, 2359-2368 (2010).
5. Brooks, B.R. et al. CHARMM: a program for macromolecular energy, minimization, and dynamics calculations. *J. Comput. Chem.* 4, 187-217 (1983).
6. MacKerell, A.D. et al. in *Encyclopedia of Computational Chemistry* (ed. Schleyer, P.) 271 (Wiley, Chicester, UK, 1998).
7. Humphrey, W., Dalke, A. & Schulten, K. VMD: Visual Molecular Dynamics. *J. Mol. Graphics* 14, 33-38 (1996).
8. Phillips, J.C. et al. Scalable molecular dynamics with NAMD. *J. Comp. Chem.* 26, 1781-1802 (2005).
9. Mackerell, A.D., Jr, Feig, M. & Brooks, C.L., III. Extending the Treatment of Backbone Energetics in Protein Force Fields: Limitations of Gas-Phase Quantum Mechanics in Reproducing Protein Conformational Distributions in Molecular Dynamics Simulations. *J. Comput. Chem.* 25, 1400-1415 (2004).
10. Jorgensen, W.L., Chandrasekhar, J., Madura, J.D., Impey, R.W. & Klein, M.L. Comparison of simple potential functions for simulating liquid water. *J. Chem. Phys.* 79, 926-935 (1983).
11. Sherwood, P. et al. QUASI: A general purpose implementation of the QM/MM approach and its application to problems in catalysis. *J. Mol. Struct. (TEOCHEM)* 632, 1-28 (2003).
12. Ahlrichs, R., Bär, M., Häser, M., Horn, H. & Kölmel, C. Electronic Structure calculation on workstation computers: The program system TURBOMOLE. *Chem. Phys. Lett.* 162, 165-169 (1989).
13. Smith, W. & Forester, T.R. DL_POLY_2.0: A general-purpose parallel molecular dynamics simulation package. *J. Mol. Graphics* 14, 136-141 (1996).

14. Grimme, S. *J. Comp. Chem.* 27, 1787-1799 (2006).

15. Becke, A.D. Density functional thermochemistry. II. The effect of the Perdew–Wang generalized gradient correlation correction. *J. Chem. Phys.* 97, 9173-9177 (1992).

16. Schäfer, A., Horn, H. & Ahlrichs, R. Fully optimized contracted Gaussian basis sets for atoms Li to Kr. *J. Chem. Phys.* 97, 2571-2577 (1992).

17. Field, M.J., Bash, P.A. & Karplus, M. A Combined Quantum Mechanical and Molecular Mechanical Potential for Molecular Dynamics Simulations. *J. Comp. Chem.* 11, 700-733 (1990).

18. Bakowies, D. & Thiel, W. *J. Phys. Chem.* 100, 10580-10594 (1996).

19. de Vries, A.H. et al. Zeolite Structure and Reactivity by Combined Quantum-Chemical-Classical Calculations. *J. Phys. Chem. B* 103, 6133-6141 (1999).

20. Antes, I. & Thiel, W. On the treatment of link atoms in hybrid methods. *ACS Symp. Ser.* 712, 50-65 (1998).

21. Billeter, S.R., Turnera, A.J. & Thiel, W. Linear scaling geometry optimisation and transition state search in hybrid delocalised internal coordinates. *Phys. Chem. Chem. Phys.* 2, 2177-2186 (2000).